

# Key Health Benefits of Korean Ueong Dry Root Extract Combined Silver Nanoparticles

Gitishree Das<sup>1</sup>, Han-Seung Shin<sup>2</sup>, Jayanta Kumar Patra<sup>1</sup>

<sup>1</sup>Research Institute of Integrative Life Sciences, Dongguk University-Seoul, Gyeonggi-do, 10326, Republic of Korea; <sup>2</sup>Department of Food Science and Biotechnology, Dongguk University-Seoul, Gyeonggi-do, 10326, Republic of Korea

Correspondence: Jayanta Kumar Patra, Research Institute of Integrative Life Sciences, Dongguk University-Seoul, Gyeonggi-do, 10326, Republic of Korea, Email jkpatra@dongguk.edu

**Introduction:** Nowadays, in nanotechnology and material science, biosynthesis of the metal nanoparticle is a promising approach.

**Methods:** In the current research, the extract of the Korean Ueong dry root (BdkR), which belongs to the *Asteraceae* family, was used as a reducing and capping agent, for the green synthesis of the BdkR-Ag nanoparticles in a cost-effective and highly efficient manner. In this study for the reaction measures, UV-Vis spectroscopy was applied. SEM, EDX, FTIR, XRD, mean size distribution, and zeta potential were used for the characterization of the green synthesized BdkR-AgNPs. In the beginning, the primary phytochemical screening of BdkR extract was estimated and the cytotoxicity, antidiabetic, antioxidant, and antibacterial activities of the green synthesized BdkR-AgNPs were evaluated.

**Results:** According to the results, the BdkR extract is rich in various phytochemicals and the generated AgNPs were crystalline in nature. The surface plasmon resonance value of the BdkR-AgNPs was 444 nm confirming the synthesis of AgNPs. The BdkR-AgNPs displayed four clear diffraction peaks at 2 theta angles (38.22); (46.15); (64.88); (76.83), respectively, which are equivalent to (111), (200), (220) and (311). The obtained nanoparticles have a zeta potential of -17.0 mV. Furthermore, the generated BdkR-AgNPs exhibited considerable antidiabetic effect in terms of the inhibition of  $\alpha$ -glucosidase with a maximum inhibition value of 95.41% at 5.0  $\mu$ g/mL and more than 86% inhibition at 2.5  $\mu$ g/mL and the estimated IC<sub>50</sub> value was found to be 0.653  $\mu$ g/mL. Further, it also displayed a significant cytotoxicity activity against the HepG<sub>2</sub> cancer cell lines at 10  $\mu$ g/mL and 100  $\mu$ g/mL concentrations with 86% and 88% of inhibition, respectively. Besides this, the synthesized AgNPs also displayed promising antioxidant activities in terms of the DPPH (IC<sub>50</sub> value - 56.26  $\mu$ g/mL), ABTS (IC<sub>50</sub> value - 171.43  $\mu$ g/mL) and reducing power (IC<sub>0.5</sub> value - 227.42  $\mu$ g/mL).

**Discussion:** The multipotential effects of the synthesized BdkR-AgNPs might be attributed to the presence of the bioactive compounds in the BdkR extract that acted as the capping and reducing agent in the synthesis process. The green synthesized BdkR-AgNPs exhibited promising bioactive potential for their future applications in the food and biomedical field.

**Keywords:** antidiabetic, antioxidant, cytotoxicity, silver nanoparticle, green synthesis

## Introduction

In the current developed disease diagnosis and treatment techniques, nano-biotechnology has become an integral part and has grown rapidly. Biogenic AgNPs are biocompatible, cost-effective, and eco-friendly, which have engrossed attention for their potential bioengineering and biomedical applications.<sup>1-4</sup> Nanoparticles are effectively used in the area of gene delivery, biomedical sciences, drug delivery, catalysis, and in chemical industries, etc.<sup>5-7</sup> Owing to strong anti-inflammatory and antibacterial potential, among other metal nanoparticles, silver nanoparticles are getting high attention. In various pharmaceutical, and biological applications, AgNPs are utilized, for example, AgNPs containing ointment or cream are useful for wounds and burn to prevent infection of bacterial, etc.<sup>6,8</sup> For the human healthy peripheral lymphocytes, AgNPs are non-toxic.<sup>9</sup> For early detection of cancer, biogenic AgNPs are used as vehicles for targeted delivery of anticancer probes or drugs.<sup>10,11</sup>

Plant-mediated silver nanoparticle synthesis has various benefits, it is of very low cost, and can be achieved under ambient temperature and the process is comparatively fast in comparison with bacteria.<sup>3</sup> Plants comprise a broad range of

metabolites that can improve in reducing silver ions, stabilizing, and capping during the synthesis of AgNPs.<sup>3,6</sup> In medicinal plants, the complex biomolecules assist in the metal ion reduction and also in the nanoparticle stabilization into preferred shape and size.<sup>6,12</sup> There are several research reports on the root mediated green synthesis of silver nanoparticles like AgNPs synthesis using *Berberis asiatica* root extract,<sup>13</sup> using *Ricinus communis* root extract,<sup>14</sup> *Astragalus tribuloides* Delile. root extract,<sup>15</sup> etc. For large production of nanoparticles, plant-mediated synthesis is a suitable, rapid, and flexible process. For the synthesis of nanoparticles currently plant parts such as leaf, bark, stem, root, latex, seed and fruit extracts, etc. were successfully used.<sup>16,17</sup> Silver NPs, among other nanoparticles, have been used enormously due to their potent antifungal, antitumor, and antibacterial activity. Silver NPs have been extensively used in the packaging of food, preservation, cosmetics, and medicine.<sup>2,16,18–20</sup>

The species of *Arctium* are well known for their various therapeutic properties due to its existence of numerous bioactive metabolites.<sup>21</sup> *Arctium lappa* belongs to the family Compositae.<sup>22</sup> It is a perennial herb that can be found globally. It is being promoted as healthy and nutritive food and therapeutically used in Asia, Europe, and North America for hundreds of years. It has been cultivated as a vegetable in Asia for a long time. Its therapeutic usages were acknowledged more than 3000 years ago in Western countries. In Europe and Asia, the BdkR plant grows in long and spindle-shaped way like a carrot reaching in thickness to the thickness of a finger and containing a large amount of potassium carbonate and potassium nitrate.<sup>23</sup> Traditionally *A. lappa* is used to treat various skin problems, rashes, boils, acne, furuncles, psoriasis, eczema, seborrheic skin, minor urinary tract disorders, sore throat, etc.<sup>21,24,25</sup> *Arctium* species contains volatile and non-volatile compounds such as aldehydes, carboxylic acids, fatty acids, hydrocarbons and lignins, acetylenic compounds, flavonoids, phytosterols, polysaccharides, etc. Even though *A. lappa* fruit, seeds, and leaves are used, but the dried root of *A. lappa* is the main part used for various therapeutic purposes.<sup>22,26</sup> It is known to have the function of draining toxins from the blood.<sup>24,27</sup> *Arctium* sp. possesses multiple biological potentials like antioxidant, antimicrobial, anti-diabetic, anticancer, antiviral, antibacterial, anti-inflammatory, anti-allergic and gastro-protective and hepato-protective, etc.<sup>24,28</sup> There is a report of remedial uses of burdock in treating diseases such as diabetes, AIDS, and cancer.<sup>24,29</sup> There is a report that the total lignan from the burdock is a safe antidiabetic agent and helps in preventing diabetic complications.<sup>24,29</sup>

Earlier research has confirmed that the BdkR contains an abundant number of bioactive compounds such as flavonoids, oligosaccharides, polyphenols, polyunsaturated fatty acids, and caffeic acid derivatives.<sup>28</sup> Currently, an increasing number of research have focused on polysaccharides extracted from burdock, particularly *fructans*, which were used as a source of insulin. Pectin (non-insulin polysaccharides) was extracted from the BdkR, and it was found to show significant anti-constipation activity.<sup>28</sup> Silver NPs synthesis using burdock root and investigation of its biological activity is very rare. It is a green method of nano synthesis. There is only a single report on the synthesis of nanoparticles using the extracts of burdock root; however, they have followed different synthesis approaches and have studied only the antimicrobial and catalytic studies.<sup>30</sup> Therefore, the use of burdock root (BdkR) in the bio-fabrication of Ag-NPs may well assist as the greatest approach for good utilization of natural herbal resources in a cost-effective and eco-friendly way. Thus, from the above perspective, the present research reports the root (BdkR) extract mediated fabrication of AgNPs, their characterization, and assessment of their various biological properties, like antioxidant, antidiabetic, and cytotoxicity action.

## Materials and Methods

### Preparation of Plant Extract

The Korean Ueong or burdock dry roots (BdkR) (Figure 1A) were obtained from the local vegetable market of Goyang-si, the Republic of Korea during August 2021. The sample was authenticated and a voucher specimen (RIILSEH No. 202108–03) has been deposited in the e-herbarium (RIILSEH), Dongguk University, Republic of Korea. The dried roots were washed with double distilled water, and with the help of tissue paper properly dried and pounded. The pounded roots (50 g) were immersed in 250 mL of double-distilled H<sub>2</sub>O in a 1 Lt of glass flask and boiled with continuous stirring (around for 30 min). Then, the mixed solution (boiled) was cooled and sieved with the help of Whatman No.1 filter paper and then put in storage at 4°C until further use.

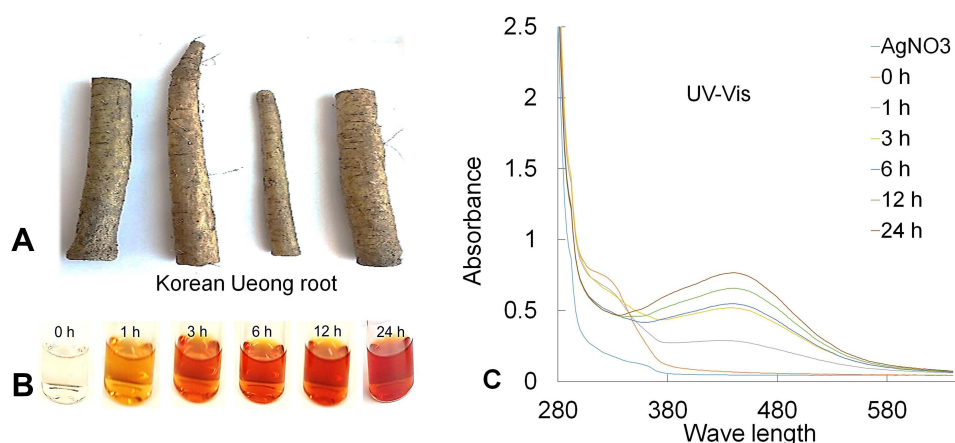


**Figure 1** Korean Ueong dry root (BdkR) (A); color change in the synthesis of BdkR-AgNPs (0–24 h) (B); UV-Vis absorbance of BdkR-AgNPs (C).

## Primary Phytochemical Screening of the Burdock Root (BdkR) Extract

The phytochemical screening of burdock or *A. lappa* root extract was done and the presence of dynamic bioactive compounds or phytochemicals such as phenolics, saponins, anthraquinones, a cardiac steroidal glycoside, carbohydrates, and flavonoids were identified using the standard procedures.<sup>31–33</sup>

## Green Synthesis and Characterization of the BdkR-AgNPs

The biosynthesis of BdkR-AgNPs was accomplished with the help of bioactive phytochemicals rich *A. lappa* root extract by using the standard protocol.<sup>5</sup> Briefly, 80 mL of the 1mM AgNO<sub>3</sub> solution was taken in a 250 mL conical flask, and to it, 20 mL of the BdkR extract was mixed slowly drop by drop with continuous stirring at room temperature. The complete synthesis of the AgNPs was recorded by monitoring the change in color of the reaction mixture followed by scanning by UV-VIS spectrophotometer. The reaction mixture was monitored for about 24 h, and then the collection of the synthesized BdkR-AgNPs was carried out by centrifugation at 12,000 rpm for 30 minutes followed by washing 3–4 times with water.

Further, the BdkR-AgNPs characterization was carried out by following six different standard analytical techniques. These analytical methods such as UV-VIS spectral study, energy-dispersive X-ray spectroscopy analysis, Fourier transform infrared spectroscopy analysis, scanning electron microscopy study, X-ray powder diffraction study, Dynamic light scattering, and zeta potential were used to characterize the BdkR-AgNPs according to standard techniques.<sup>5,34,35</sup> The preliminary synthesis of the BdkR-AgNPs was confirmed by scanning between 300 and 700 nm using the UV-VIS spectrophotometer (Multiskan Go; Thermo Scientific, Waltham, MA, USA). The morphology of the synthesized BdkR-AgNPs was characterized by the SEM machine (Hitachi S-3000N, Tokyo, Japan) and the elemental composition was determined by an EDX machine attached to the SEM. The FT-IR spectra of both BdkR-AgNPs and the BdkR extract were evaluated at wavelengths ranging between 400 and 4000 cm<sup>-1</sup> by using the FT-IR spectrophotometer (ThermoFisher Scientific, USA). The nature of the BdkR-AgNPs was characterized by using the XRD machine at a set-up of Cu K $\alpha$  radians at 40 mA and 30 kV at an angle of 2 $\theta$  (Panalytical, The Netherlands). The size distribution (Dynamic Light Scattering) and Zeta potential of the BdkR-AgNPs were characterized by Malvern Zetasizer Nano-ZS machine, Malvern, UK, machine.

## Cytotoxicity Effect of BdkR-AgNPs

The BdkR-AgNPs cytotoxicity effect against the HepG<sub>2</sub> cancer cells was valued through a kit (EZ Cytotoxicity Assay Kit, Do-Gen-Bio Co., Limited, Seoul, The Republic of Korea) by using the company's manufacture method. The HepG<sub>2</sub> cancerous cells were procured from the Korean Cell Line Bank, Seoul, and the Republic of Korea. The test samples (BdkR-AgNPs) were diluted (at 1000  $\mu$ g/mL concentration) through a filter of 0.22 $\mu$ m (syringe filter, Millipore, Billerica, USA). The live cell

% (Cell viability) and also the cell configuration exposed to the generated BdkR-AgNPs was calculated by the trypan blue exclusion investigation method.<sup>36</sup> The OD of BdkR-Ag nanoparticle (in DMEM solution) was checked in between (the range of 300–700 nm) wavelength before the HepG2 cancer cell line treatment. The supernatant was replaced by a new medium or solution of (110 µL) comprise EZ-Cytox (10 µL solution) after 24 h of exposition and kept (incubated around twenty minutes) till the melon-red shade transformed to yellowish-orange color. After incubation, the BdkR-AgNPs testers (samples) were relocated in a separate plate (96 wells). Next, the resultant absorbance value remained recorded at 450 nm wavelength, using a spectrophotometer (Spectra Max 384 Plus; Sunnyvale, CA, USA). Further, the cell sustainability (the viability of cell) of cancer (HepG<sub>2</sub>) cell lines treated with the synthesized BdkR-Ag nanoparticles was evaluated by the trypan blue exclusion test.

Further, after exposing the cells for 24 h, the supernatant was removed and the cell lines were washed immediately with 100 µL (DPBS). Next, freshly prepared whole DMEM and trypan blue mix solution in a ratio of 1:1 (20 µL) was added to every well. At that point, the viability of the cell was detected through a microscope (Inverted microscope, DM16000B, Leica, Wetzlar, Germany).<sup>36</sup>

## Evaluation of the Antidiabetic Effect of BdkR-AgNPs

The α-glucosidase inhibition (antidiabetic potential) effect of BdkR-Ag nanoparticles was evaluated by following the standard method of Butala et al.<sup>37</sup> The generated BdkR-AgNPs were liquefied (using methanol in a sonicated water bath). The test sample BdkR-AgNPs (10 µg/mL) was transferred to a plate of 96 well then with sodium phosphate buffer diluted serially (0.02 M, P<sup>H</sup> 6.9). Next, α-glucosidase (0.5 U/mL) was added to a final volume of 50 µL to each. It is next incubated for 10 min at room temperature. Then, 50 µL of the substrate was taken (3.0 mM P-nitrophenyl-glucopyranoside). The reaction solution was kept for 20 min at 37°C for incubation. To the reaction mix (solution) an aliquot of (50 µL of Na<sub>2</sub>CO<sub>3</sub>, 0.1 M) was added, and at 405 nm wavelength, the absorbance value was documented. The percentage of inhibition was estimated using the below formula.

$$\text{Inhibition \%} = \frac{C_r - T_r}{C_r} \times 100$$

Here, C<sub>r</sub> is the value (control absorbance value) of, T<sub>r</sub> is the value (tested sample absorbance value).

## Evaluation of the Antioxidant Effect of BdkR-AgNPs

The antioxidant effect of the synthesized BdkR-Ag nanoparticle was calculated by DPPH, ABTS, and reducing power scavenging (free radical) assays using the standard technique.<sup>34</sup> In brief, the BdkR-AgNPs scavenging effect in DPPH assay and BHT was used as standard control (using methanol) as control blank. The absorbance of the solution (reaction mix) was taken as standard control by taking methanol as the control blank. By a UV-visible spectrum (Multiskan Go Spectrophotometer; Thermo Scientific, Waltham, MA, USA) study, the absorbance value of the solution (reaction mix) was estimated and the result was calculated as per equation (1).

$$\text{DPPH free radical scavenging effect percentage} = \frac{C_r - T_r}{C_r} \times 100 \quad (1)$$

Where C<sub>r</sub> is (control absorbance value) and T<sub>r</sub> is (tested sample absorbance value).

ABTS free radical scavenging potential of BdkR-AgNPs was evaluated by the standard procedure using BHT as the reference standard.<sup>34</sup> The scavenging potential was calculated as per equation (1). The BdkR-AgNPs, reducing power assay was estimated by using the earlier protocol (standard) of.<sup>34</sup> The reducing power potential was estimated at 700 nm by the absorbance result of the solution (reaction mix).

## Statistical Study

The statistical study of generated BdkR-AgNPs was carried out using ANOVA (one way) by following Duncan's multiple tests by statistical analysis SPSS (software version 25.0 and IBM Crop, Armonk, NY, USA), at 5% significance level (P < 0.05). The obtained result is exhibited as the mean of the three values by standard deviation.

## Results and Discussion

### Green Fabrication and Characterization of BdkR-AgNPs

Metals like Ag have a very strong surface plasmon resonance, which is vital in the synthesis of nanoparticles. Physical methods require high-energy consumption in the synthesis process of nanoparticles, and usually, in the chemical method of the synthesis process, it leads to the generation of some toxic reactions and resulted in the no use of produced nanoparticles in biological applications. Thus, many researchers have selected green-synthesis of NPs using biocompatible sources like plants, bacteria, fungi, etc. which can be a greater substitute to other chemical approaches as it is non-toxic, safe, and economical biocompatible.<sup>38,39</sup> Further, the chemical methods have many disadvantages over the green synthesis method as the chemical synthesis methods use toxic chemicals, it releases hazardous by-products, generates aggregated large-sized particles, time consumption is higher and less stable, etc. as it uses chemicals this is toxic to the human body.<sup>38</sup> The green-nanoparticle synthesis process is extremely reliable as it is free from toxic substances. However, there are still few reports on the toxic effect of green synthesized silver NPs.<sup>40</sup> So still, it is essential to do a safety survey in detail that for humans, green synthesized NPs are free of side effects. In this context, the current investigation is safe as BdkR root extract, which is usually used as food in most parts of the world, is used for the synthesis of AgNPs. For nanoparticle synthesis, the usage of plants offers an extensive range of profits over the other biosynthesis methods since it does not require any maintenance and supports large-scale nanoparticle synthesis. Biosynthesis of AgNPs using plant extracts having phytochemical agents has fascinated considerable interest. The Ag nanoparticles have many applications in eye disease therapy, wound healing, pharmaceuticals, and other applications.<sup>41</sup>

The current study carried out the green synthesis of BdkR-AgNPs by the dry root of *Arctium lappa* (Burdock) extracts. In this research, the phytochemical screening of the BdkR extract was carried out to know the presence of various types of bioactive phytochemicals such as flavonoids, terpenoids, tannins, saponins, carbohydrates, phenolics, etc. The BdkR-AgNPs were bio-generated using the BdkR extract, which was enriched with several phytochemicals like saponins, terpenoids, flavonoids, proteins and amino acids, cardiac steroidal glycoside steroids, and carbohydrates (Table 1). These phytochemicals played a significant role in the reduction, capping, and stabilization of the BdkR-AgNPs during the synthesis process. A previous study on the green synthesis of silver nanoparticles has proved that the phytochemicals such as phenolic acids and flavonoids present in the plant extract act as the reducing agents and the phytochemicals such as the xanthenes and phloroglucinols act as the capping agents, and another compound, naphthodianthrone are involved in both the steps.<sup>42</sup> This also proves our claim of the role of the phytochemicals in the synthesis of the BdkR-AgNPs.<sup>42,43</sup> Through visual assessment of the reaction mix (reaction solution) in terms of the shift of the pigment to brown color, the BdkR-Ag nanoparticle synthesis was confirmed (Figure 1B).<sup>20,44</sup>

Next to visual confirmation of the solution (test reaction) the variation in the pigment of the solution (reaction), the BdkR-AgNPs reaction solution was exposed to a spectrophotometer for analysis. The UV-VIS spectrophotometric investigation outcome of BdkR-AgNPs solution (test reaction) was documented at constant time intermissions (up to 24 h) (Figure 1C).

**Table 1** Preliminary Phytochemical Screening of *A. lappa* Root Aqueous Extract

Name of Phytochemicals	The Reaction of <i>A. lappa</i> Root Extract
Flavonoids	+
Terpenoids	+
Saponins	+
Steroids	++
Proteins & Amino acids	+++
Carbohydrates	+++
Anthraquinones	-
Cardiac steroidal glycoside	+

**Notes:** + = Present; and - = Absent.



Generally owing to the free electrons, Ag nanoparticles display a surface plasmon resonance (SPR) value in between 440 and 558 nm.<sup>45</sup> By the UV-VIS spectrum study, the BdkR-AgNPs reaction kinetics was tracked (from 280 to 650 nm). Upon excitation, the oscillatory motion of the electrons in silver has headed to collisions, unveiling the surface plasma resonance (SPR) bands that are the characteristic feature of AgNPs as detected in UV-Vis spectroscopy.<sup>19</sup> The SPR value of the BdkR-AgNPs shows a peak value at 444 nm wavelength (Figure 1C) which confirms the synthesis of BdkR-AgNPs and it is also similar to the previously reported AgNPs synthesis results.<sup>20,46</sup> The change in the color of the BdkR-AgNPs solution can be linked with the excitation process of the surface plasmon vibration within the biologically synthesized BdkR-AgNPs as evident from the previously published literature.<sup>4,47</sup> This optical property of the synthesized BdkR-AgNPs is usually sensitive to concentration, shape, size, and the agglomeration state of the synthesized nanoparticles.<sup>48</sup> Further, the above values signify that the phytochemicals present in the BdkR extracts act as reducing and capping elements.<sup>49–52</sup>

The BdkR-AgNPs morphology and basic configuration were studied through SEM and EDX analysis. The generated BdkR-AgNPs, SEM analysis result was based on nanometer-scale imaging (Figure 2A) and it was confirmed that the

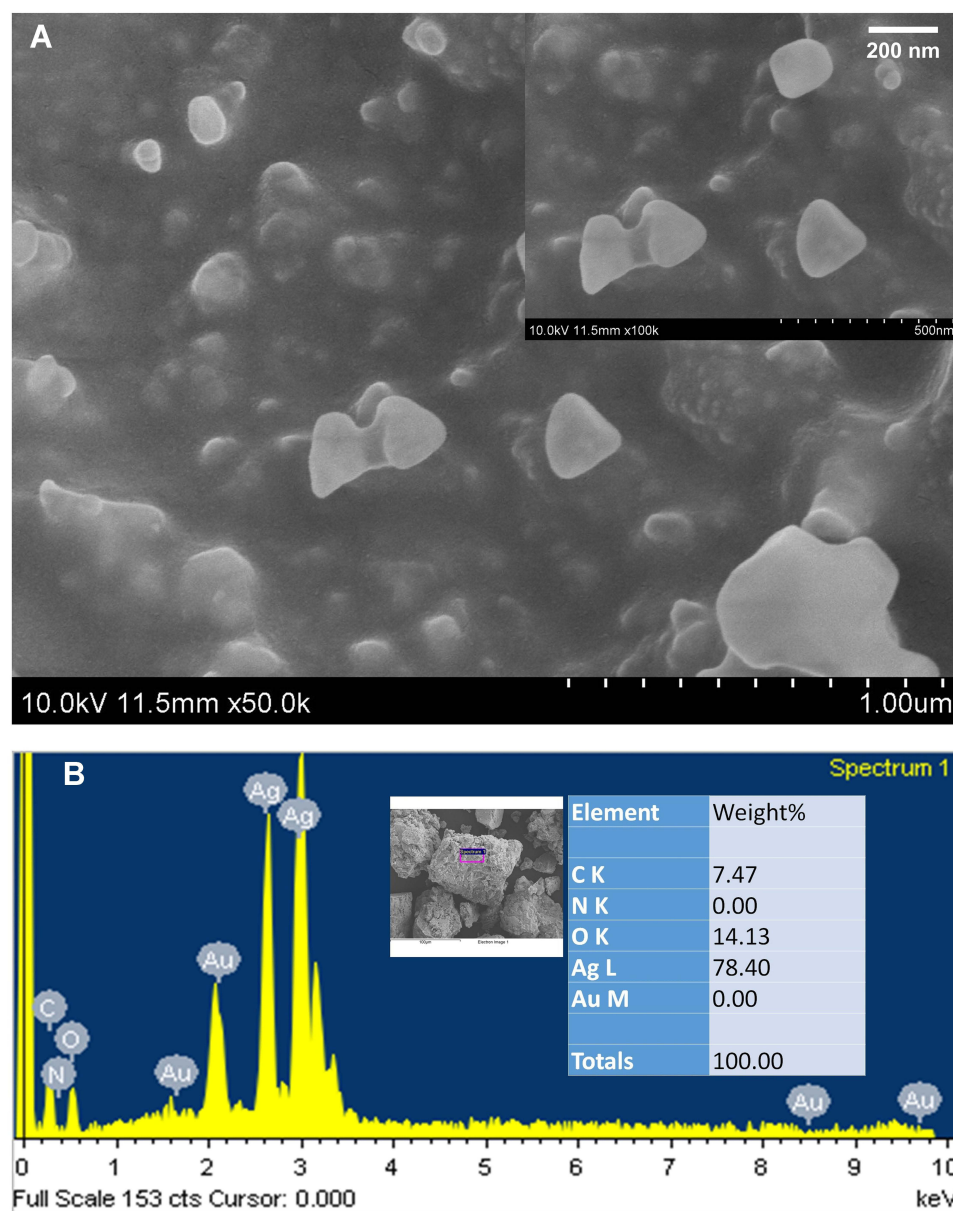


**Figure 2** SEM image of BdkR-AgNPs (A), EDX spectra of BdkR-AgNPs (inset, elemental percentage) (B).

generated BdkR-AgNPs were analogous to what has been specified earlier.<sup>53,54</sup> Besides, the average particle size as calculated using the ImageJ software from the SEM image was found to be 72.656 nm. The elemental structure of the generated BdkR-AgNPs was obtained by the EDX analysis, which displayed the presence of the Ag (78.40%), C (7.47%), and O (14.13%) (Figure 2B). The EDX result presented a graph that displayed the main peak value detecting the presence of the silver (Ag, 78.40%) component (Figure 2B, inset). Further, in Figure 2B, the EDX analysis data showed a strong signal around the 3 keV for elemental silver and the residue of other elements that are attached to the surface of the BdkR-AgNPs. Besides, two other peaks are showing the presence of carbon and oxygen which might be due to the presence of bioactive compounds from the BdkR extract which was used as the capping and reducing agent in the synthesis of BdkR-AgNPs.<sup>4</sup> These results are similar to other previously published literature.<sup>19,55,56</sup>

The BdkR-AgNPs, XRD evaluation revealed the generated AgNPs physical sketch and also showed the BdkR-AgNPs crystalline nature and nanostructure from the noticeable peaks (Figure 3) which is equal to the face-centered cubic phase of Ag<sub>0</sub> standard JCPDS card no. 04–0783 (fcc).<sup>57</sup> The BdkR-AgNPs displayed four clear diffraction peaks at 2 theta angles (38.22); (46.15); (64.88); (76.83), respectively, which are equivalent to (111), (200), (220) and (311) was documented (Figure 3). The above-witnessed peaks are probably owing to the existence of bioactive phyto-compounds in the BdkR extract, which is similar to the earlier research report.<sup>20,38</sup>

The identification of the functional groups present in the BdkR extract was done by FTIR analysis of the BdkR extract and BdkR-AgNPs. The shift of the compounds witnessed in BdkR-AgNPs proposes their dynamic involvement in the green synthesis of Ag nanoparticles.<sup>20</sup> The BdkR extract and BdkR-AgNPs FTIR results exhibited various stretching modes with various peak values (Figure 4). The BdkR extract peak values at 3306.32, 2105.37, 1634.03, 1081.63, and 691.37 cm<sup>-1</sup> possibly shifted to 3310.09, 2114.79, 1630.26, 1132.64, and 605.71 cm<sup>-1</sup> in case of BdkR-AgNPs

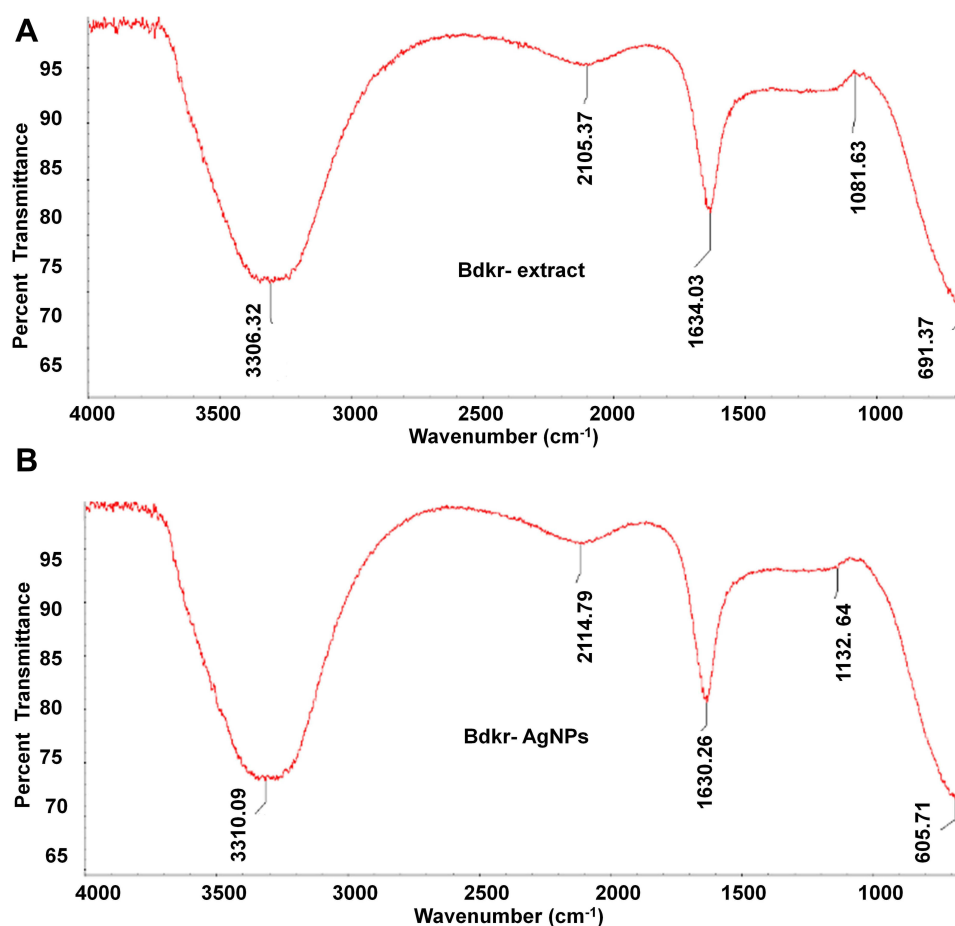


**Figure 3** FTIR data of Bdkr-extract (A) and BdkR-AgNPs (B).

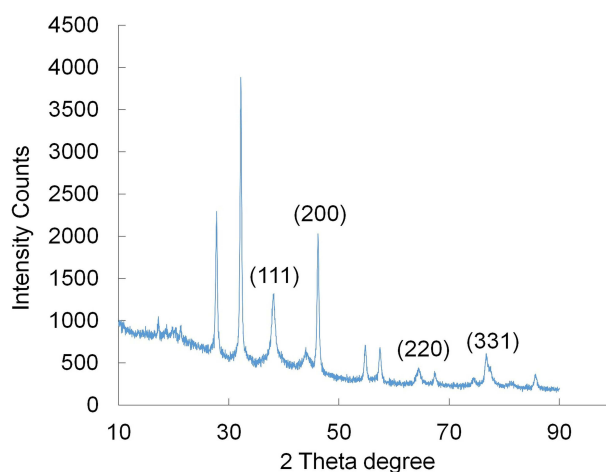


**Figure 4** XRD results of BdkR-AgNPs.

(Figure 4). The BdkR-AgNPs peak at  $3310.09\text{ cm}^{-1}$  indicates the existence of O–H bond, H-bonding stretching belong to alcohols and phenols functional groups.<sup>58</sup> The peak at  $2114.79\text{ cm}^{-1}$  designates the appearance of the  $\text{--C}\equiv\text{C--}$  bond, which comes under the alkynes groups. The resultant peak at  $1630.26\text{ cm}^{-1}$  specifies the presence of N–H bonds, which come under amine (primary) functional groups. The resultant value at  $1132.64\text{ cm}^{-1}$  the peak specifies the presence of C–O/C–N stretch, which comes under the esters, alcohols, carboxylic acids, and ethers or the aliphatic amines functional group. The absorption at  $605.71\text{ cm}^{-1}$  indicates the presence of C–Br stretch which comes under the alkyl halides functional group.<sup>58</sup> It was also found that when the peaks of both the BdkR extract and BdkR-AgNPs were compared there was a significant modification in the peak at  $691.37\text{ cm}^{-1}$  that was found in the BdkR extract but was shifted towards  $605.71\text{ cm}^{-1}$  in the case of the BdkR-AgNPs, and as a result, the presence of  $\text{--C}\equiv\text{C--H}$ : C–H bend which corresponds to the alkynes has disappeared from the BdkR-AgNPs (Table 2). The slight deviation in the absorption peak value of the BdkR extract and BdkR-Ag nanoparticles could be credited to capping and stabilizing processes throughout the green synthesis of BdkR-AgNPs.<sup>57</sup> The analogous result has been reported in the earlier research.<sup>20,59–61</sup>

It has been reported that the morphology and polydispersity of the AgNPs can be stabilized by the optimal reaction conditions and the reducing agents such as the primary metabolites—proteins, organic acids, polysaccharides—and secondary metabolites—flavonoids and alkaloids.<sup>19,62</sup> Besides, the functional groups present in the biomolecules of the synthesized BdkR-AgNPs

**Table 2** FTIR Peaks of BdkR Extract and BdkR-AgNPs and the Corresponding Vibrational and Functional Groups

Extracts	Peaks	Vibrational Groups	Functional Groups
BdkR extract	3306.32,	O–H bond, H-bonding	Alcohols and phenols
	2105.37,	$\text{--C}\equiv\text{C--}$ bond	Alkynes
	1634.03,	N–H bonds	1° amine
	1081.63, and	C–O/C–N stretch	Esters, alcohols, carboxylic acids, and ethers or the aliphatic amines
	$691.37\text{ cm}^{-1}$	C–Br/ $\text{--C}\equiv\text{C--H}$ : C–H bend	Alkyl halides or alkynes
BdkR-AgNPs	3310.09	O–H bond, H-bonding	Alcohols and phenols
	2114.79,	$\text{--C}\equiv\text{C--}$ bond	Alkynes
	1630.26,	N–H bonds	1° amine
	1132.64,	C–O/C–N stretch	Esters, alcohols, carboxylic acids, and ethers or the aliphatic amines
	$605.71\text{ cm}^{-1}$	C–Br stretch	Alkyl halides



could attribute to the stabilization of the colloidal suspension by acting as the capping/stabilizing and reducing agents as detected as the multiple peaks on the spectrum of FTIR analysis. The particle size, dynamic light scattering measurement, and the zeta potential of the BdkR-AgNPs were used to find the average size of BdkR-AgNPs (Figure). The Z-average was found to be 170.3nm with a 0.336 PDI value (Figure 5A). It has been proved that the Zeta potential with either the high negative value or the high positive value showed a propensity to repel each other, thus lessening the agglomeration of the NPs.<sup>4,63</sup> In the current case, the polydispersed nature of the BdkR-AgNPs is due to the high negative zeta potential that prevents the formation of agglomerates resulting in maintaining the stability of the material. The obtained nanoparticles have a zeta potential equal to  $-17.0$  mV (Figure 5B, inset).

## Investigation of BdkR-AgNPs Antidiabetic, Cytotoxicity, and Antioxidant Potential

### Analysis of the Antidiabetic Effect of BdkR-AgNPs

The generated BdkR-AgNPs was found to be having a remarkable antidiabetic effect by showing maximum inhibition (95.41%) at  $5.0$   $\mu\text{g/mL}$  and more than 86% inhibition against  $\alpha$ -glucosidase at  $2.5$   $\mu\text{g/mL}$  tested concentration and the estimated  $\text{IC}_{50}$  value was very low ( $0.653$   $\mu\text{g/mL}$ ) as displayed in Table 3 and Figure 6A. The green synthesized BdkR-Ag nanoparticles exhibited a better effect than the previously stated research on green synthesized Ag nanoparticles.<sup>64</sup> The BdkR-AgNPs also displayed a similar effect of Ag nanoparticles for inhibition of  $\alpha$ -glucosidase has been detailed previously by Govindappa et al.<sup>65</sup> The substantial antidiabetic effect of the BdkR-AgNPs is witnessed from its much lower  $\text{IC}_{50}$  value (Table 3).

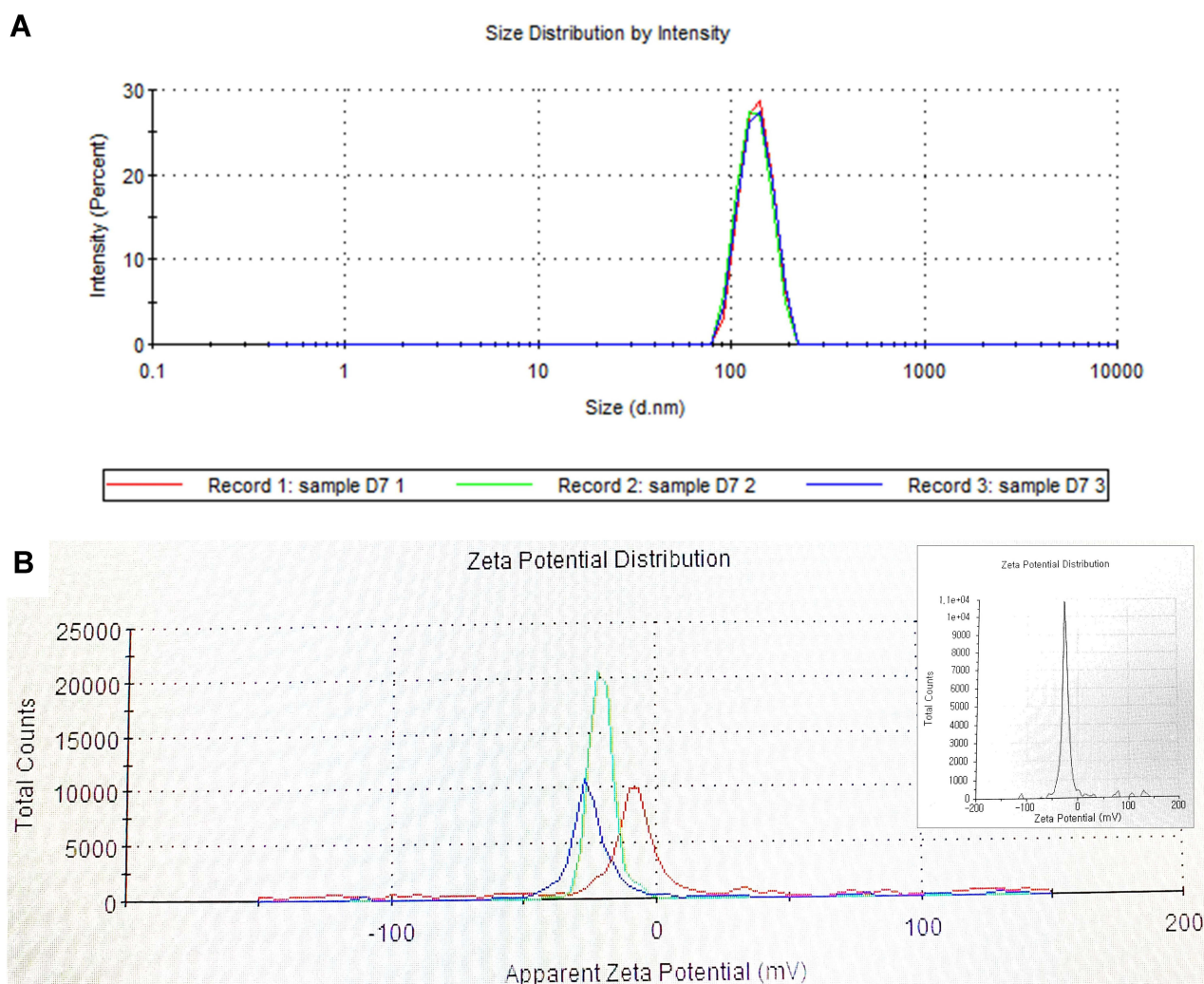


**Figure 5** DLS and Zeta potential analysis of BdkR-AgNPs. Size distribution (**A**) and zeta potential analysis (inset zeta potential) (**B**).

**Table 3** Antioxidant and Antidiabetic Studies of BdkR-AgNPs (IC<sub>50</sub> Values)

Parameters	IC <sub>50</sub> Value (µg/mL) BdkR-AgNPs	BHT (µg/mL)
DPPH	56.27 µg/mL	66.51 µg/mL
ABTS	171.43 µg/mL	40.24 µg/mL
Reducing	*227.42 µg/mL	*108.54 µg/mL
Antidiabetic (α-glucosidase)	0.653 µg/mL	NA

Note: \*IC<sub>0.5</sub> value.

### Analysis of Cytotoxicity Effect of BdkR-AgNPs

Worldwide, currently cancer claims the lives of millions of people annually. Consequently, in the past few years, the development of therapeutics from natural products has considerably increased.<sup>66</sup> The cytotoxicity ability of Ag is due to the bioactive physicochemical interaction of silver particles with functional groups of intracellular proteins, as well as the phosphate groups and nitrogen bases in DNA.<sup>67</sup> In the current study, the green synthesized BdkR Ag nanoparticles exhibited significant cytotoxicity activity against cancer cell lines (HepG<sub>2</sub>). The unique structure of nanoparticles offers them an exclusive potential to target the unusual cancerous cell growth activated as a result of neoplastic alteration. In the detection and management of cancer-associated syndromes, nano-drugs have been identified to be greatly effective.<sup>44,68</sup> The BdkR-AgNPs cytotoxicity effect has a size and dose-

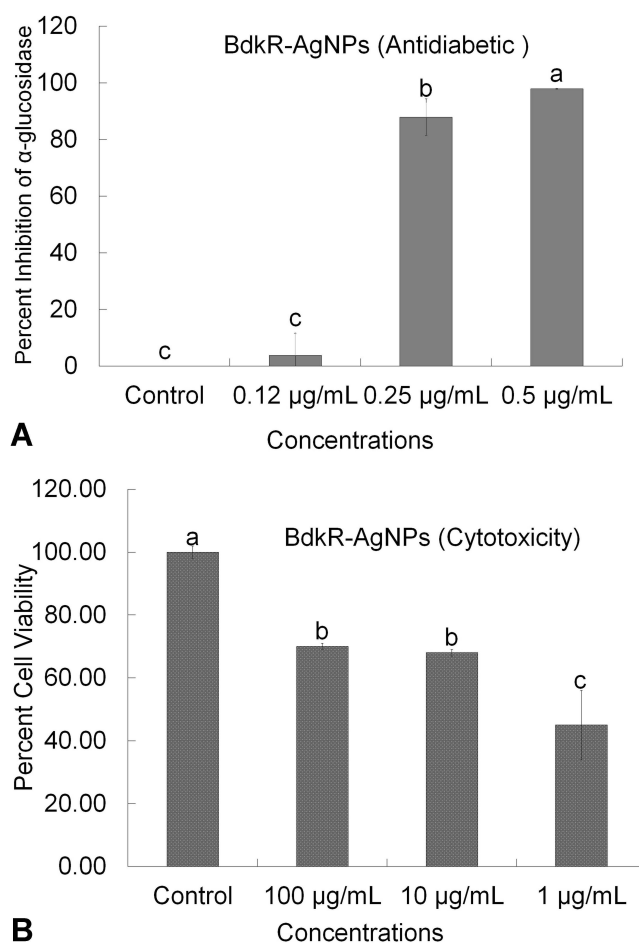


**Figure 6** Antidiabetic potential (α-glucosidase) of BdkR-AgNPs (**A**); cytotoxicity (cell viability %) result of BdkR-AgNPs (**B**).

dependent consequence. The green synthesized Ag nanoparticles cytotoxicity effect might be dependent on various factors such as Ag nanoparticle distribution of size, shape, and exterior chemistry. The alteration in these components might lead to a change in cytotoxicity response.<sup>69,70</sup> The AgNPs inactivate the activity of ATPase, prepare the cell signaling, and in conclusion lead to apoptosis.<sup>71</sup> As well, in the physical or chemical methods of nanoparticle synthesis commonly poisonous substances are used which are naturally deadly and raise several side effects. Therefore, these nanoparticles are not suggested for use in biomedical applications. Therefore, green synthesized NPs are preferred for biomedical applications of nanoparticles that are non-toxic and eco-friendly.<sup>72</sup> In the current research, the resultant diagram of the viability of the cell revealed that the amount of HepG<sub>2</sub> (live) cell was greater as the concentration of the BdkR-AgNPs decreased (Figure 5). The treated HepG<sub>2</sub> cancer cells with different concentrations BdkR-AgNPs were noticed using an inverted light microscope. The highest concentration of the BdkR-AgNPs was substantially toxic to HepG<sub>2</sub> cancer cell lines. The live-cell line ratio was higher when the treatment concentration of the BdkR-AgNPs was reduced (Figure 6B). The green synthesized BdkR-Ag nanoparticles exhibited significant cytotoxicity effect against cancer (HepG<sub>2</sub>) cell line (Figure 6B). The BdkR-AgNPs were highly active at 10 µg/mL and 100 µg/mL concentrations with 86% and 88% of inhibition, respectively (Figure 5). Earlier, it was detailed that just after arriving the cell by the course of phagocytosis, endocytosis, or diffusion, the Ag nanoparticle by itself or by the ionized Ag<sup>+</sup> produces the reactive oxygen species which creates the oxidative stress.<sup>73</sup> In this study, the cytotoxicity effect of the synthesized BdkR-AgNPs is analogous or higher than the previous research reports.<sup>44,70,74</sup> The electrostatic attraction in between nanoparticles and cells also plays an important role in cytotoxicity effect of Ag nanoparticles.<sup>67</sup>

### Analysis of the Antioxidant Effect of BdkR-AgNPs

The antioxidant analyses like DPPH, ABTS, and reducing power study through three tested concentrations (25, 50, and 100 µg/mL) of BdkR-AgNPs results presented in Figure 7. All three tested assay results are concentration-dependent. The antioxidant effect was better with the increase in the concentration of the BdkR-AgNPs. The antioxidant effect was higher

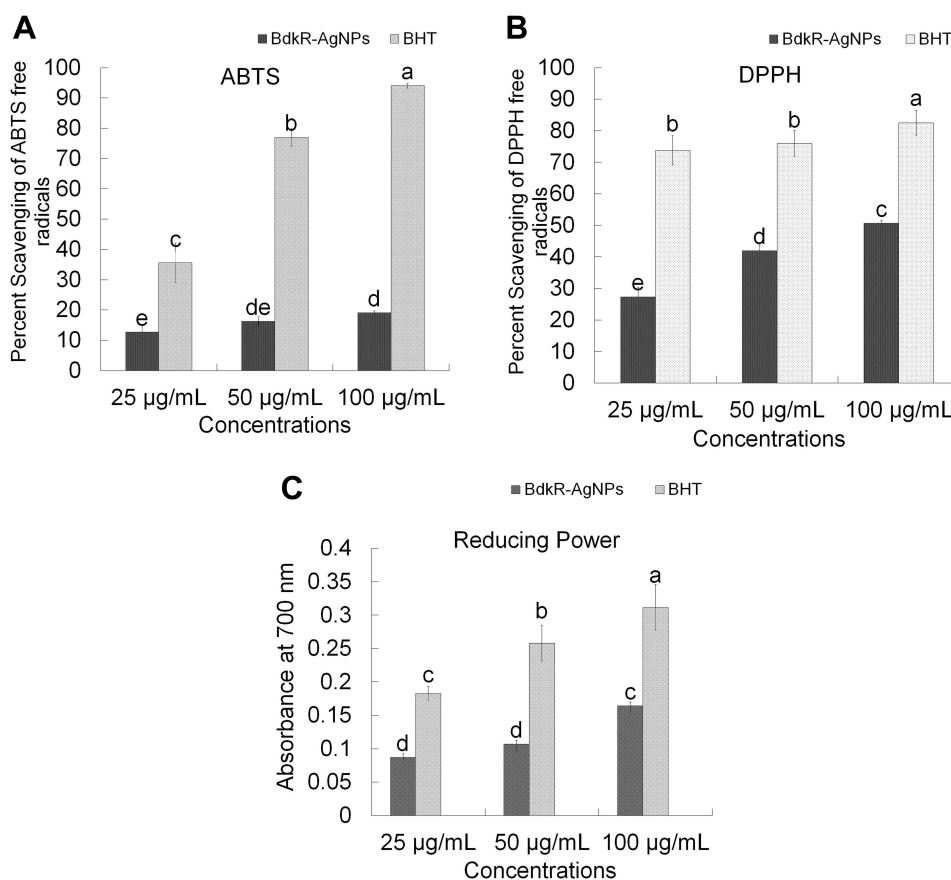


**Figure 7** Antioxidant potential of BdkR-AgNPs. (A) ABTS assay; (B) DPPH assay; (C) reducing power assay.

in the DPPH assay than ABTS and reducing power assays of BdkR-AgNPs (Figure 7). As a whole, the generated BdkR-AgNPs exhibited a modest antioxidant effect (Figure 7). The DPPH scavenging activity of BdkR-AgNPs displayed a higher effect than the ABTS scavenging effect, which is parallel to the earlier stated research report.<sup>75</sup> The antioxidant assays IC<sub>50</sub> values are presented in Table 3. From the three free radical scavenging effect assay it was concluded that the BdkR-AgNPs have a moderate antioxidant effect, which is similar or lower with the previous reports.<sup>64,75</sup> The result might be due to the phytochemicals present in BdkR extract, which played an important role in the process of capping and stabilizing Ag nanoparticles.<sup>76</sup> The phytochemicals that exist in the BdkR root extract act as a major role in antioxidant potential. The antioxidant parameters like DPPH assay showed the IC<sub>50</sub> value of 56.26 µg/mL for BdkR-AgNPs and 66.51 µg/mL for the standard BHT, for ABTS assay, the IC<sub>50</sub> value of BdkR-AgNPs is 171.43 µg/mL and it was 40.24 µg/mL in case of the standard BHT. In the case of the reducing power assay, the IC<sub>0.5</sub> value of BdkR-AgNPs was found to be 227.42 µg/mL and 108.54 µg/mL for the standard BHT (Table 3). It is reported that the overproduction of highly reactive, usually unstable, and capable of initiating the chain reactions of free radicals due to an inequality in the oxidation-reduction equilibrium has led to stress and cell death-related diseases.<sup>4,19</sup> It is of utmost importance to suppress or neutralize these free radicals, and in this case, the current BdkR-AgNPs with promising antioxidant potential could be very much helpful.

## Conclusion

In the green or biosynthesis process of BdkR-AgNPs, the bioactive component of BdkR extract plays a substantial role as a capping and reducing agent. The green synthesized BdkR-AgNPs seem to be an appropriate candidate for the management of diabetes, cancer and can be well utilized in related biomedical applications. It is concluded that the phytofabrication method adopted in the current investigation is a one-step rapid and simple procedure, and is amenable in the scaling up for the large-scale production of AgNPs in a cost-effective way. This non-toxic biosynthesis of BdkR-AgNPs exhibited promising bioactive potential with many future applications.

## Acknowledgment

G Das, H-S Shin, and JK Patra are grateful to Dongguk University-Seoul, the Republic of Korea for the support. This work was supported by the National Research Foundation of Korea (NRF) grant funded by the Korean Government (MSIT) (No. 2020R1G1A1004667), the Republic of Korea.

## Author Contributions

G Das, H-S Shin, and JK Patra made a significant contribution in the conception, study design, execution, acquisition of data, analysis, and interpretation; and took part in drafting, revising, and critically reviewing the article; gave final approval of the version to be published; have agreed on the journal to which the article has been submitted; and agreed to be accountable for all aspects of the work.

## Funding

This work was supported by the National Research Foundation of Korea (NRF) grant funded by the Korean government (MSIT) (No. 2020R1G1A1004667), the Republic of Korea.

## Disclosure

The authors declare that there is no conflict of interest exists with this manuscript.

## References

1. Ratan ZA, Haidere MF, Nurunnabi M, et al. Green chemistry synthesis of silver nanoparticles and their potential anticancer effects. *Cancers*. 2020;12(4):855. doi:10.3390/cancers12040855
2. Raj S, Trivedi R, Soni V. Biogenic synthesis of silver nanoparticles, characterization and their applications—a review. *Surfaces*. 2022;5(1):67–90. doi:10.3390/surfaces5010003
3. Mustapha T, Misni N, Ithnin NR, Daskum AM, Unyah NZ. A review on plants and microorganisms mediated synthesis of silver nanoparticles, role of plants metabolites and applications. *Int J Environ Res Public Health*. 2022;19(2):674. doi:10.3390/ijerph19020674



4. Sharma A, Sagar A, Rana J, Rani R. Green synthesis of silver nanoparticles and its antibacterial activity using fungus *Talaromyces purpureogenus* isolated from *Taxus baccata* Linn. *Micro Nanosyst Letters*. 2022;10(1):1–12. doi:10.1186/s40486-022-00144-9
5. Irvani S, Korbekandi H, Mirmohammadi SV, Zolfaghari B. Synthesis of silver nanoparticles: chemical, physical and biological methods. *Res Pharm Sci*. 2014;9(6):385.
6. Urmukhsaikhan E, Bold B-E, Gunbileg A, Sukhbaatar N, Mishig-Ochir T. Antibacterial activity and characteristics of silver nanoparticles biosynthesized from *carduus crispus*. *Scientific Reports*. 2021;11. doi:10.1038/s41598-021-00520-2
7. Ssekatawa K, Byarugaba DK, Angwe MK, et al. Phyto-mediated copper oxide nanoparticles for antibacterial, antioxidant and photocatalytic performances. *Front Bioeng Biotechnol*. 2022;10. doi:10.3389/fbioe.2022.820218
8. Khandel P, Shahi SK, Soni DK, Yadav RK, Kanwar L. *Alpinia calcarata*: potential source for the fabrication of bioactive silver nanoparticles. *Nano Converg*. 2018;5(1):1–17. doi:10.1186/s40580-018-0167-9
9. Gengan R, Anand K, Phulukdaree A, Chuturgoon A. A549 lung cell line activity of biosynthesized silver nanoparticles using *Albizia adianthifolia* leaf. *Colloids Surf B Biointerfaces*. 2013;105:87–91. doi:10.1016/j.colsurfb.2012.12.044
10. Locatelli E, Naddaka M, Uboldi C, et al. Targeted delivery of silver nanoparticles and alisertib: in vitro and in vivo synergistic effect against glioblastoma. *Nanomedicine*. 2014;9(6):839–849. doi:10.2217/nnm.14.1
11. Hossain MM, Polash SA, Takikawa M, et al. Investigation of the antibacterial activity and in vivo cytotoxicity of biogenic silver nanoparticles as potent therapeutics. *Front Bioeng Biotechnol*. 2019;7:239. doi:10.3389/fbioe.2019.00239
12. Natsuki J, Natsuki T, Hashimoto Y. A review of silver nanoparticles: synthesis methods, properties and applications. *Int J Mater Sci Appl*. 2015;4(5):325–332. doi:10.11648/j.ijmsa.20150405.17
13. Dangi S, Gupta A, Gupta DK, Singh S, Parajuli N. Green synthesis of silver nanoparticles using aqueous root extract of *Berberis asiatica* and evaluation of their antibacterial activity. *Chem Data Coll*. 2020;28:100411. doi:10.1016/j.cdc.2020.100411
14. Gul A, Shaheen F, Shaheen A, et al. Green synthesis, characterization, enzyme inhibition, antimicrobial potential, and cytotoxic activity of plant mediated silver nanoparticle using *ricinus communis* leaf and root extracts. *Biomolecules*. 2021;11(2):206. doi:10.3390/biom11020206
15. Sharifi-Rad M, Pohl P, Epifano F, Álvarez-suarez JM. Green synthesis of silver nanoparticles using *Astragalus tribuloides delile*. root extract: characterization, antioxidant, antibacterial, and anti-inflammatory activities. *Nanomaterials*. 2020;10(12):2383. doi:10.3390/nano10122383
16. Paulkumar K, Gnanajobitha G, Vanaja M, et al. *Piper nigrum* leaf and stem assisted green synthesis of silver nanoparticles and evaluation of its antibacterial activity against agricultural plant pathogens. *Sci World J*. 2014;2014:1–9. doi:10.1155/2014/829894
17. Ahmed RH, Mustafa DE. Green synthesis of silver nanoparticles mediated by traditionally used medicinal plants in Sudan. *Int Nano Lett*. 2020;10(1):1–14. doi:10.1007/s40089-019-00291-9
18. Jeevanandam J, Krishnan S, Hii YS, et al. Synthesis approach-dependent antiviral properties of silver nanoparticles and nanocomposites. *J NANOSTRUCTURE CHEM*. 2022. 1–23. doi:10.1007/s40097-021-00465-y
19. Chandrasekharan S, Chinnasamy G, Bhatnagar S. Sustainable phyto-fabrication of silver nanoparticles using *Gmelina arborea* exhibit antimicrobial and biofilm inhibition activity. *Sci Rep*. 2022;12(1):1–16. doi:10.1038/s41598-021-04025-w
20. Ahmad N, Fozia F, Jabeen M, et al. Green fabrication of silver nanoparticles using *Euphorbia serpens* Kunth aqueous extract, their characterization, and investigation of its *in vitro* antioxidative, antimicrobial, insecticidal, and cytotoxic activities. *Biomed Res Int*. 2022;2022:5562849. doi:10.1155/2022/5562849
21. Wang D, Bădărau AS, Swamy MK, et al. *Arctium* species secondary metabolites chemodiversity and bioactivities. *Front Plant Sci*. 2019;10:834. doi:10.3389/fpls.2019.00834
22. Zhang X, Herrera-Balandrano DD, Huang W, et al. Comparison of nutritional and nutraceutical properties of burdock roots cultivated in fengxian and peixian of China. *Foods*. 2021;10(9):2095. doi:10.3390/foods10092095
23. Hossein MH, Sedaghat S. Green synthesis and morphological investigation of silver nanoparticles using greater burdock (*Arctium lappa*) Aqueous extracts. *Pak. J Med. Health Sci*. 2018;12(4):1839–1844.
24. Chan Y-S, Cheng L-N, Wu J-H, et al. A review of the pharmacological effects of *Arctium lappa* (burdock). *Inflammopharmacology*. 2011;19(5):245–254. doi:10.1007/s10787-010-0062-4
25. Miglani A, Manchanda RK. Observational study of *Arctium lappa* in the treatment of acne vulgaris. *Homeopathy*. 2014;103(3):203–207. doi:10.1016/j.homp.2013.12.002
26. Miazga-Karska M, Michalak K, Ginalska G. Anti-acne action of peptides isolated from burdock root—preliminary studies and pilot testing. *Molecules*. 2020;25(9):2027. doi:10.3390/molecules25092027
27. Yu B-S, Yan X-P, Xiong J, Xin Q. Simultaneous determination of chlorogenic acid, forsythidin and arctiin in Chinese traditional medicines preparation by reversed phase-HPLC. *Chem Pharm Bull (Tokyo)*. 2003;51(4):421–424. doi:10.1248/cpb.51.421
28. Watanabe A, Sasaki H, Miyakawa H, Nakayama Y, Lyu Y, Shibata S. Effect of dose and timing of burdock (*Arctium lappa*) root intake on intestinal microbiota of mice. *Microorganisms*. 2020;8(2):220. doi:10.3390/microorganisms8020220
29. Xu Z, Wang X, Zhou M, et al. The antidiabetic activity of total lignan from *Fructus Arctii* against alloxan-induced diabetes in mice and rats. *Phytother Res*. 2008;22(1):97–101. doi:10.1002/ptr.2273
30. Nguyen TT-N, Vo -T-T, Nguyen BN-H, et al. Silver and gold nanoparticles biosynthesized by aqueous extract of burdock root, *Arctium lappa* as antimicrobial agent and catalyst for degradation of pollutants. *Environ Sci Pollut Res*. 2018;25(34):34247–34261. doi:10.1007/s11356-018-3322-2
31. Sofowora A. Medicinal plants and medicine in Africa. John Wiley Spectrum, Ibadan Nigeria; 1993: 281–285.
32. Ravikumar V, Gopal V, Sudha T. Analysis of phytochemical constituents of stem bark extracts of *Zanthoxylum tetraspermum* Wight & Arn. *Res J Pharmaceut Biol Chem Sci*. 2012;3(4):391–402.
33. Gul R, Jan SU, Faridullah S, Sherani S, Jahan N. Preliminary phytochemical screening, quantitative analysis of alkaloids, and antioxidant activity of crude plant extracts from *ephedra intermedia* indigenous to Balochistan. *Sci World J*. 2017;2017:1–7. doi:10.1155/2017/5873648
34. Zhou Y, Itoh H, Uemura T, Naka K, Chujo Y. Preparation of  $\pi$ -conjugated polymer-protected gold nanoparticles in stable colloidal form. *Chem Commun*. 2001;7:613–614. doi:10.1039/b100636n
35. Patra JK, Shin H-S, Das G. Characterization and evaluation of multiple biological activities of silver nanoparticles fabricated from dragon tongue bean outer peel extract. *Int J Nanomedicine*. 2021;16:977. doi:10.2147/IJN.S290037
36. Faedmaleki F, Shirazi FH, Salarian -A-A, Ashtiani HA, Rastegar H. Toxicity effect of silver nanoparticles on mice liver primary cell culture and HepG2 cell line. *Iran J Pharm Res*. 2014;13(1):235–242.



37. Butala MA, Kukkupuni SK, Venkatasubramanian P, Vishnuprasad CN. An ayurvedic anti-diabetic formulation made from *Curcuma longa* L. and *Embolica officinalis* L. Inhibits  $\alpha$ -Amylase,  $\alpha$ -Glucosidase, and starch digestion, in vitro. *Starch-Stärke*. 2018;70(5–6):1700182. doi:10.1002/star.201700182
38. Behravan M, Panahi AH, Naghizadeh A, Ziaee M, Mahdavi R, Mirzapour A. Facile green synthesis of silver nanoparticles using *Berberis vulgaris* leaf and root aqueous extract and its antibacterial activity. *Int J Biol Macromol*. 2019;124:148–154. doi:10.1016/j.ijbiomac.2018.11.101
39. Hawar SN, Al-Shmangani HS, Al-Kubaisi ZA, Sulaiman GM, Dewir YH, Rikisahedew JJ. Green synthesis of silver nanoparticles from alhagi graecorum leaf extract and evaluation of their cytotoxicity and antifungal activity. *J Nanomater*. 2022;2022:1–8. doi:10.1155/2022/1058119
40. Dobrucka R, Szymanski M, Przekop R. The study of toxicity effects of biosynthesized silver nanoparticles using *Veronica officinalis* extract. *Int J Environ Sci Technol*. 2019;16(12):8517–8526. doi:10.1007/s13762-019-02441-0
41. Chung I-M, Park I, Seung-Hyun K, Thiruvengadam M, Rajakumar G. Plant-mediated synthesis of silver nanoparticles: their characteristic properties and therapeutic applications. *Nanoscale Res Lett*. 2016;11(1):40. doi:10.1186/s11671-016-1257-4
42. Pradeep M, Kruska D, Kachlicki P, Mondal D, Franklin G. Uncovering the phytochemical basis and the mechanism of plant extract-mediated eco-friendly synthesis of silver nanoparticles using ultra-performance liquid chromatography coupled with a photodiode array and high-resolution mass spectrometry. *ACS Sustain Chem Eng*. 2022;10(1):562–571. doi:10.1021/acsschemeng.1c06960
43. Bawazeer S, Rauf A, Shah SUA, et al. Green synthesis of silver nanoparticles using *Tropaeolum majus*: phytochemical screening and antibacterial studies. *Green Process Synth*. 2021;10(1):85–94. doi:10.1515/gps-2021-0003
44. Oves M, Aslam M, Rauf MA, et al. Antimicrobial and anticancer activities of silver nanoparticles synthesized from the root hair extract of *Phoenix dactylifera*. *Mater Sci Eng C*. 2018;89:429–443. doi:10.1016/j.msec.2018.03.035
45. Khalil MM, Ismail EH, El-Baghady KZ, Mohamed D. Green synthesis of silver nanoparticles using olive leaf extract and its antibacterial activity. *Arab J Chem*. 2014;7(6):1131–1139. doi:10.1016/j.arabjc.2013.04.007
46. Saravanan M, Barik SK, MubarakAli D, Prakash P, Pugazhendhi A. Synthesis of silver nanoparticles from *Bacillus brevis* (NCIM 2533) and their antibacterial activity against pathogenic bacteria. *Microb Pathog*. 2018;116:221–226. doi:10.1016/j.micpath.2018.01.038
47. Awwad AM, Salem NM, Abdeen AO. Green synthesis of silver nanoparticles using carob leaf extract and its antibacterial activity. *Int J Indust Chem*. 2013;4(1):1–6. doi:10.1186/2228-5547-4-29
48. Widatalla HA, Yassin LF, Alrasheid AA, et al. Green synthesis of silver nanoparticles using green tea leaf extract, characterization and evaluation of antimicrobial activity. *Nanoscale Adv*. 2022;4(3):911–915. doi:10.1039/D1NA00509J
49. John S, Monica J, Priyadarshini S, Sivaraj C, Arumugam P. Antioxidant and Antibacterial activities of *Beta vulgaris* L. Peel extracts. *Int J Pharma Res Health Sci*. 2017;5(6):1974–1979. doi:10.21276/ijprhs.2017.06.14
50. Elsorady M, Ali S. Antioxidant activity of roasted and unroasted peanut skin extracts. *Int Food Res J*. 2018;25(1):43–50.
51. Araújo RG, Rodriguez-Jasso RM, Ruiz HA, Pintado MME, Aguilar CN. Avocado by-products: nutritional and functional properties. *Trends Food Sci Technol*. 2018;80:51–60. doi:10.1016/j.tifs.2018.07.027
52. Mirmiran P, Houshalsadat Z, Gaeini Z, Bahadoran Z, Azizi F. Functional properties of beetroot (*Beta vulgaris*) in management of cardio-metabolic diseases. *Nutr Metab*. 2020;17(1):1–15. doi:10.1186/s12986-019-0421-0
53. Velmurugan P, Sivakumar S, Young-Chae S, et al. Synthesis and characterization comparison of peanut shell extract silver nanoparticles with commercial silver nanoparticles and their antifungal activity. *J Ind Eng Chem Res*. 2015;31:51–54. doi:10.1016/j.jiec.2015.06.031
54. Soto KM, Quezada-Cervantes CT, Hernández-Iturriaga M, Luna-Bárcenas G, Vazquez-Duhalt R, Mendoza S. Fruit peels waste for the green synthesis of silver nanoparticles with antimicrobial activity against foodborne pathogens. *LWT*. 2019;103:293–300. doi:10.1016/j.lwt.2019.01.023
55. Palithya S, Gaddam SA, Kotakadi VS, Penchalaneni J, Challagundla VN. Biosynthesis of silver nanoparticles using leaf extract of *Decaschistia crotonifolia* and its antibacterial, antioxidant, and catalytic applications. *Green Chem Lett Rev*. 2021;14(1):137–152. doi:10.1080/17518253.2021.1876172
56. He X, Luan F, Zhao Z, et al. The genus *Patrinia*: a review of traditional uses, phytochemical and pharmacological studies. *Am J Chin Med*. 2017;45(04):637–666. doi:10.1142/S0192415X17500379
57. He Y, Wei F, Ma Z, et al. Green synthesis of silver nanoparticles using seed extract of *Alpinia katsumadai*, and their antioxidant, cytotoxicity, and antibacterial activities. *RSC Adv*. 2017;7(63):39842–39851. doi:10.1039/C7RA05286C
58. Coates J. Interpretation of infrared spectra, a practical approach; 2000.
59. de Barros CHN, Cruz GCF, Mayrink W, Tasic L. Bio-based synthesis of silver nanoparticles from Orange waste: effects of distinct biomolecule coatings on size, morphology, and antimicrobial activity. *Nanotechnol Sci Appl*. 2018;11:1. doi:10.2147/NSA.S156115
60. Antony E, Sathivelu M, Arunachalam S. Synthesis of silver nanoparticles from the medicinal plant *Bauhinia acuminata* and *Biophytum sensitivum*—a comparative study of its biological activities with plant extract. *Int J Appl Pharm*. 2017;9(1):1–8.
61. Netala VR, Kotakadi VS, Nagam V, Bobbu P, Ghosh SB, Tartte V. First report of biomimetic synthesis of silver nanoparticles using aqueous callus extract of *Centella asiatica* and their antimicrobial activity. *Appl Nanosci*. 2015;5(7):801–807. doi:10.1007/s13204-014-0374-6
62. Singh P, Kim Y-J, Zhang D, Yang D-C. Biological synthesis of nanoparticles from plants and microorganisms. *Trends Biotechnol*. 2016;34(7):588–599. doi:10.1016/j.tibtech.2016.02.006
63. Singh T, Jyoti K, Patnaik A, Singh A, Chauhan R, Chandel S. Biosynthesis, characterization and antibacterial activity of silver nanoparticles using an endophytic fungal supernatant of *Raphanus sativus*. *J Genet Eng Biotechnol*. 2017;15(1):31–39. doi:10.1016/j.jgeb.2017.04.005
64. Chinnasamy G, Chandrasekharan S, Bhatnagar S. Biosynthesis of silver nanoparticles from *Melia azedarach*: enhancement of antibacterial, wound healing, antidiabetic and antioxidant activities. *Int J Nanomedicine*. 2019;14:9823. doi:10.2147/IJN.S231340
65. Govindappa M, Hemashekhar B, Arthikala M-K, Rai VR, Ramachandra Y. Characterization, antibacterial, antioxidant, antidiabetic, anti-inflammatory and antityrosinase activity of green synthesized silver nanoparticles using *Calophyllum tomentosum* leaves extract. *Results Phys*. 2018;9:400–408. doi:10.1016/j.rinp.2018.02.049
66. Khandelwal R, Arora S, Phase D, Pareek A. Anti cancer potential of green synthesized silver nanoparticles. Paper presented at: AIP Conference Proceedings; 2020, 020046 (2020).
67. Karimi S, Shahri MM. Medical and cytotoxicity effects of green synthesized silver nanoparticles using *Achillea millefolium* extract on MOLT-4 lymphoblastic leukemia cell line. *J Med Virol*. 2020;93:3899–3906.
68. Pugazhendhi A, Edison TNJI, Karuppusamy I, Kathirvel B. Inorganic nanoparticles: a potential cancer therapy for human welfare. *Int J Pharm*. 2018;539(1–2):104–111. doi:10.1016/j.ijpharm.2018.01.034

69. Qian L, Su W, Wang Y, Dang M, Zhang W, Wang C. Synthesis and characterization of gold nanoparticles from aqueous leaf extract of *Alternanthera sessilis* and its anticancer activity on cervical cancer cells (HeLa). *Artif Cells, Nanomed Biotechnol.* **2019**;47(1):1173–1180. doi:10.1080/21691401.2018.1549064
70. Barabadi H, Vahidi H, Kamali KD, Rashedi M, Saravanan M. Antineoplastic biogenic silver nanomaterials to combat cervical cancer: a novel approach in cancer therapeutics. *J Cluster Sci.* **2020**;31(4):659–672. doi:10.1007/s10876-019-01697-3
71. Tang J, Lu X, Chen B, et al. Mechanisms of silver nanoparticles-induced cytotoxicity and apoptosis in rat tracheal epithelial cells. *J Toxicol Sci.* **2019**;44(3):155–165. doi:10.2131/jts.44.155
72. Roy N, Gaur A, Jain A, Bhattacharya S, Rani V. Green synthesis of silver nanoparticles: an approach to overcome toxicity. *Environ Toxicol Pharmacol.* **2013**;36(3):807–812. doi:10.1016/j.etap.2013.07.005
73. Akter M, Sikder MT, Rahman MM, et al. A systematic review on silver nanoparticles-induced cytotoxicity: physicochemical properties and perspectives. *J Adv Res.* **2018**;9:1–16. doi:10.1016/j.jare.2017.10.008
74. Hemlata H, Meena PR, Singh AP, Tejavath, KK. Biosynthesis of silver nanoparticles using *Cucumis prophetarum* aqueous leaf extract and their antibacterial and antiproliferative activity against cancer cell lines. *ACS omega.* **2020**;5(10):5520–5528. doi:10.1021/acsomega.0c00155
75. Otunola GA, Afolayan AJ. In vitro antibacterial, antioxidant and toxicity profile of silver nanoparticles green-synthesized and characterized from aqueous extract of a spice blend formulation. *Biotechnol Biotechnol Equip.* **2018**;32(3):724–733. doi:10.1080/13102818.2018.1448301
76. Adedapo AA, Jimoh FO, Afolayan AJ, Masika PJ. Antioxidant activities and phenolic contents of the methanol extracts of the stems of *Acokanthera oppositifolia* and *Adenia gummifera*. *BMC Complement Altern Med.* **2008**;8(1):54. doi:10.1186/1472-6882-8-54

## International Journal of Nanomedicine

Dovepress

### Publish your work in this journal

The International Journal of Nanomedicine is an international, peer-reviewed journal focusing on the application of nanotechnology in diagnostics, therapeutics, and drug delivery systems throughout the biomedical field. This journal is indexed on PubMed Central, MedLine, CAS, SciSearch®, Current Contents®/Clinical Medicine, Journal Citation Reports/Science Edition, EMBase, Scopus and the Elsevier Bibliographic databases. The manuscript management system is completely online and includes a very quick and fair peer-review system, which is all easy to use. Visit <http://www.dovepress.com/testimonials.php> to read real quotes from published authors.

Submit your manuscript here: <https://www.dovepress.com/international-journal-of-nanomedicine-journal>